



ELSEVIER

Contents lists available at SciVerse ScienceDirect

# Journal of Quantitative Spectroscopy & Radiative Transfer

journal homepage: [www.elsevier.com/locate/jqsrt](http://www.elsevier.com/locate/jqsrt)

## Diode laser spectroscopy of methyl fluoride overtones at 850 nm

Q1 A. Lucchesini\*, S. Gozzini

Istituto Nazionale di Ottica - CNR - U.O.S. "Adriano Gozzini" Area della Ricerca - Via G. Moruzzi, 1 - 56124 Pisa, Italy

### ARTICLE INFO

#### Article history:

Received 23 January 2013

Received in revised form

18 March 2013

Accepted 21 March 2013

#### Keywords:

Methyl fluoride

Overtone bands

Line and band widths

Tunable diode laser

Symmetric top molecule

### ABSTRACT

One hundred fifty-six  $^{12}\text{CH}_3\text{F}$  overtone absorption lines, comprised between 11 545 and 11 836  $\text{cm}^{-1}$ , have been observed by using a tunable diode laser (TDL) spectrometer. Their intensities range around  $10^{-26}$  cm/molecule and have been measured by utilizing commercial AlGaAs/GaAs laser diodes through the wavelength modulation (WM) and the 2nd harmonic (2f) detection techniques. Self-broadening coefficients and line strengths have been measured at room temperature for seven of the strongest transitions, while air-broadening coefficients have been obtained for two lines. In addition, self- and air-collisional shifts have been measured for the 11 564.25  $\text{cm}^{-1}$  transition.

© 2013 Published by Elsevier Ltd.

### 1. Introduction

$\text{CH}_3\text{F}$  (methyl fluoride) is a symmetric top molecule very much investigated by conventional spectroscopic techniques as well as by the more sophisticated Fourier transform infrared (FTIR) spectrometers. It has a large permanent dipole moment, which explains the large self-collisional absorption line-broadening as it happens for ammonia [1,2]. Since some of  $\text{CO}_2$  laser lines coincide with some resonances of the fundamental  $\nu_3$  vibrational absorption band of  $\text{CH}_3\text{F}$ , this has been at first studied by using the  $\text{CO}_2$  laser as the source, by means of the Stark shift spectroscopy [3]. Later on, the use of the semiconductor tunable laser sources [4] widened the range of the spectroscopic investigation.

$\text{CH}_3\text{F}$  overtones and combination of vibrational fundamentals in the near infrared (NIR) in the gas phase have been observed by Thompson [5] early in 1939. Later on the fifth overtone spectra of the C–H stretching vibrations of

methyl fluoride (fluoro-methane) have been located at 15 972  $\text{cm}^{-1}$  by using the intracavity dye laser photoacoustic spectroscopy [6]. More recently a systematic study of the overtone spectra of methyl halides,  $\text{CH}_3\text{F}$  included, has been carried on the 4 and 5 quanta of C–H stretching excitation by a FTIR spectrometer [7].

We focalized our attention to the ro-vibrational overtones and combinations located in the wavelength range between 845 and 865 nm, covered by our diode laser spectrometer. In particular this spectral interval covers the tail of the 4 quanta of C–H stretching excitation ( $4\nu_{\text{C-H}}$ ) and probably the superposition of the two combinations  $3\nu_{\text{C-H}} + 2\nu_2$  and  $3\nu_{\text{C-H}} + 2\nu_5$  in analogy with what happens to  $\text{CH}_3\text{Cl}$  [8]. In this ro-vibrational high energy range it is very difficult to assign the absorption lines to the right quanta of vibration and rotation, ought to the many overlapping bands whose upper states are often coupled by various interactions, such as the Fermi and the Coriolis resonances [9]. Moreover the weakness of these absorption lines forced the use of long path cells and noise reduction techniques. From this viewpoint the availability of the laser diodes (LDs) facilitates the use of the wavelength modulation spectroscopy (WMS) technique to increase the signal-to-noise (S/N) ratio.

\* Corresponding author. Tel.: +39 050 6212533; fax: +39 050 3152247.  
E-mail address: [lucchesini@ino.it](mailto:lucchesini@ino.it) (A. Lucchesini).

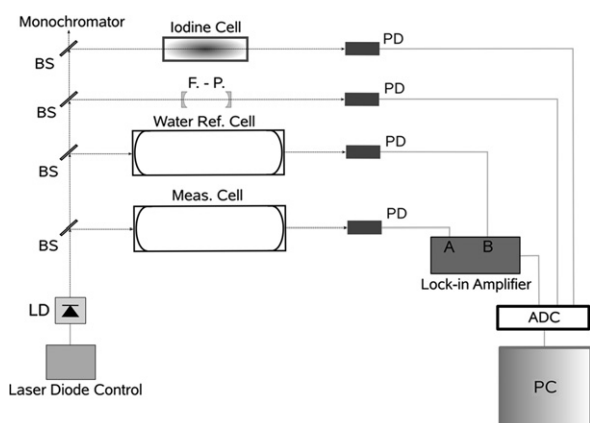


**Fig. 1.** Outline of the experimental apparatus. ADC: analog-to-digital converter; BS: beam splitter; F.-P.: Fabry-Perot interferometer; LD: laser diode; M: mirror; PC: desk-top computer; PD: photodiode.

By the aid of the LD and the WMS we observed almost 160  $\text{CH}_3\text{F}$  absorption lines and we measured also the self-broadening coefficients for seven of the more intense of them; in addition, for the most intense line at  $11\,564.25\text{ cm}^{-1}$  the self- and air-shift coefficients have been obtained.

## 2. Experimental details

The experimental setup for the WMS with the 2nd harmonic detection technique follows what was used in a previous work [10].

In particular, referring to Fig. 1, the employed source at first was a Roithner Mod. RLT85100G AlGaAs/GaAs heterostructure LD, which nominally emits 120 mW cw at 845–855 nm. Its emission has a longitudinal and transverse single mode. It was adopted in the part of the  $\text{CH}_3\text{F}$  absorption spectrum between  $11\,795$  and  $11\,836\text{ cm}^{-1}$ . Thereafter the Thorlabs LP850P030 index-guided multiple quantum well LD has been utilized. It emits 30 mW cw monomodal radiation in a range of 840–860 nm and it was used here to cover the spectrum from  $11\,545$  to  $11\,780\text{ cm}^{-1}$ . They were in turn mounted in a “free-running” configuration, that is without any electronic or optical feedback. In this condition the LDs measured emission line-widths were within 50 MHz for both of them. By varying the LDs temperatures and injection currents, as explained in the followings, we covered a total of  $300\text{ cm}^{-1}$  (more than 20 nm), even if the LDs mode hops obscured part of this range. They were hosted in a small vacuum chamber, with a Brewster angle glass exit window. The vacuum was necessary to avoid any water condensation when working at low temperature and to better stabilize the LD temperature by eliminating the convection. It is well known that LD temperature control is critical as its typical emission wavelength regime is about 0.1 nm/K. In this experimental configuration the temperature could be changed from 277 K to 323 K by using a Peltier junction mounted in direct contact to the LD housing. The fine linewidth control was guaranteed by a fine and accurate current regulation within  $\pm 10\ \mu\text{A}$  as the LD emission characteristic slope is about 0.01 nm/mA.



**Fig. 2.** A particular of the laser diode beam reflections on one of the two mirrors of the multipass Herriott type cell.

Another critical issue for the right utilization of the LDs in spectroscopy is related to their big solid angle emission divergence ( $20^\circ \times 30^\circ$ ), therefore the right choice of a good collimating lens can improve their performance. In this case we put an antireflection coated lens of small focal length close to the LD emission edge, in order to collect as much as possible emission radiation and to obtain a good quality TEM<sub>00</sub> laser beam for some meters path length.

The other important components of the spectrometer were the two 30 m path-length multipass cells, Herriott type (S.I.T. S.r.l., Mod. MPC-300 [11]), one containing the sample gas and the other containing water at vapor pressure  $\approx 20$  Torr: this second cell was used both for checking the eventual presence of water in the measurement cell, and contemporary as the reference for the precise wavenumber measurements through the utilization of the absorption lines database HITRAN [12]. Fig. 2, obtained by an infrared camera, exhibits the particular of the reflection spots on one mirror in the measurement cell.

In the region where there was a lack of tabulation of the water vapor absorption lines, an iodine reference glass cell was also used for the same purpose by referring to a specific atlas [13]. Unfortunately in some cases the iodine lines were too weak to be detected by the system, and therefore some  $\text{CH}_3\text{F}$  absorption lines could not be measured and they are not reported here. A confocal 5 cm Fabry-Perot (F.-P.) interferometer (f.s.r. = 1.5 GHz,  $0.05\text{ cm}^{-1}$ ) was utilized to check the amount and the linearity of the LD emission frequency variation obtained by sweeping the LD injection current. A 0.35 m focal length Czerny-Turner monochromator MacPherson EU-700 was used for the rough wavelength check ( $\pm 0.01\text{ nm}$ ). The methyl fluoride pure gas was supplied by Matheson Tri Inc., with purity  $\geq 99\%$ :  $\text{N}_2 \leq 150\text{ ppm}$ ,  $\text{O}_2 \leq 50\text{ ppm}$ ,  $\text{H}_2\text{O} \leq 20\text{ ppm}$ ,  $\text{N}_2 \leq 10\text{ ppm}$ . A capacitive pressure gauge (Varian, Model 6543-25-045) was connected directly to the measurement cell in order to make precise measurements ( $\pm 0.5\text{ Torr}$ ).

In this experiment the transmittance  $\tau(\nu)$  has been measured following the expression of Lambert-Beer:

$$\tau(\nu) = e^{-\sigma(\nu)z}, \quad (1)$$

where  $z = \rho l$  is the product of the absorbing species density  $\rho$  (in molecule/ $\text{cm}^3$ ) and the optical path  $l$  (in cm) of the radiation through the sample, in practice

the column amount (in molecule/cm<sup>2</sup>), and  $\sigma(\nu)$  is the absorption cross section (in cm<sup>2</sup>/molecule).

All the experiments object of this work developed in small optical depth regime, that is  $\sigma(\nu)z \ll 1$ , therefore the following approximation of Eq. (1) has been adopted:

$$\tau(\nu) \approx 1 - \sigma(\nu)z. \quad (2)$$

### 2.1. Wavelength modulation

The WMS technique applied here has been described in detail in a previous work [2]. Summarizing, the emission frequency of the source  $\bar{\nu}$  is sinusoidally modulated at the frequency  $\nu_m = \omega_m/2\pi$  (in this case  $\sim 5$  kHz) through the injection current, and results in

$$\nu = \bar{\nu} + a \cos \omega_m t. \quad (3)$$

$$f_2(x, m) = \frac{2}{m^2} - \frac{2^{1/2}}{m^2} \times \frac{1/2[(M^2 + 4x^2)^{1/2} + 1 - x^2][(M^2 + 4x^2)^{1/2} + M]^{1/2} + |x|[(M^2 + 4x^2)^{1/2} - M]^{1/2}}{(M^2 + 4x^2)^{1/2}}, \quad (6)$$

The transmitted intensity depends on both the line shape and the modulation parameter; here the utilization of the phase detection technique, obtained by a lock-in amplifier tuned to double the modulation frequency ( $\sim 10$  kHz) permits to get the 2nd harmonic signal. The  $2f$  detection has the advantage of a flat baseline of the signal and the final sensitivity is limited neither by the detector noise nor by the source noise, but by the étalon effect fringe patterns coming principally from the multipass cell mirrors.

For a low modulation amplitude  $a$ , that is  $a/\Gamma \ll 1$ , where  $\Gamma$  is the line width, the signal revealed by the lock-in amplifier gives a measurement comparable to the second derivative of the absorption feature.

Here all the experiments were carried on at pressures ranging between 20 and 300 Torr. In these conditions the absorption line shape as a function of the photon energy (frequency) can be well described by the Voigt function, a convolution of the Gaussian (Doppler width: *inhomogeneous* broadening) and Lorentzian (collisional width: *homogeneous* broadening) functions:

$$f(\nu) = \int_{-\infty}^{+\infty} \frac{\exp[-(t-\nu_0)^2/\Gamma_G^2 \ln 2]}{(t-\nu)^2 + \Gamma_L^2} dt, \quad (4)$$

where  $\nu_0$  is the gas resonance frequency,  $\Gamma_G$  and  $\Gamma_L$  are the Gaussian and the Lorentzian half widths at half the maximum (HWHM), respectively.

Eventual velocity changing collision effects, like the Dicke narrowing that occurs when the molecular mean free path is comparable to the wavelength of the sampling radiation [14], were not observed in our measurement conditions, at least within our sensitivity, and were not taken into account here.

A nonlinear least-squares fit procedure explained elsewhere [15] has been used in order to extract the line parameters and the relative errors. In particular, for the line broadening measurements the general expression of the collisional full width at half the maximum (FWHM) as

a function of the pressure has been used:

$$w_c(p) = 2\Gamma_L(p) = \gamma_i p_i + \gamma_{\text{self}} p_0, \quad (5)$$

where  $p$  is the total pressure,  $p_0$  is the partial pressure of the sample gas,  $p_i$  is partial pressure of the buffer gas  $i$ ,  $\gamma_i$  is the FWHM broadening coefficient related to the buffer gas, and  $\gamma_{\text{self}}$  is the sample gas self-broadening coefficient.

The eventual systematic instrumental distortion was checked from the self-broadening linear fit, whether the intercept to  $p=0$  always gave the  $\Gamma_L = 0$  within the laser diode emission line-width, that is 50 MHz.

In case of high modulation amplitude, the second derivative of the Voigt function cannot describe the right line-shape behavior any more and a different approach is necessary. As explained in Ref. [2], in particular in the Appendix, the spectroscopic parameters can be still obtained with a good reliability by using the following fit function of the  $2f$  signal:

where  $x = \nu/\Gamma$  and  $M = 1 - x^2 + m^2$ .

By adopting these procedures 156 CH<sub>3</sub>F absorption lines have been detected and their wavenumbers measured within 0.01 cm<sup>-1</sup> (maximum error:  $3\sigma$ ) in both the reference cases: water vapor and iodine. The absorption cross sections were on the order of 10<sup>-25</sup> cm<sup>2</sup>/molecule, which corresponds to the line strength  $S \sim 10^{-26}$  cm/molecule.

An example of a spectrum obtained near the limit of sensitivity of the spectrometer is shown in Fig. 3, which displays the CH<sub>3</sub>F at 11 836.30 cm<sup>-1</sup> and the H<sub>2</sub>O at 11 836.46 cm<sup>-1</sup> absorption lines at room temperature. The lines are broadened by modulation, the modulation index being  $m = a/\Gamma = 1.6$ . The methyl fluoride partial pressure was 32 Torr, while the water vapor pressure in its measurement cell was 19 Torr. The lock-in amplifier band-width was 10 Hz. The small étalon effect was

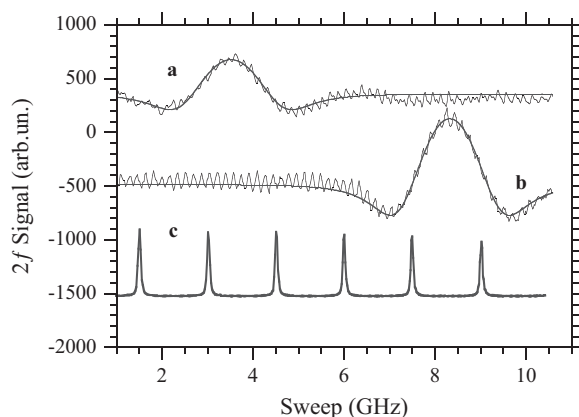


Fig. 3. Second harmonic absorption signal of CH<sub>3</sub>F (a) and H<sub>2</sub>O (b) around 844.6 nm obtained by WMS with 10 Hz bandwidth, along with the best peak fit.  $p_{\text{CH}_3\text{F}} = 32$  Torr,  $p_{\text{H}_2\text{O}} = 19$  Torr,  $T = 293$  K. The transmission of the F-P. interferometer (f.s.r. = 1.5 GHz) is shown (c) as frequency marker.

**Table 1**Wavenumbers ( $\nu'$ ) and wavelengths ( $\lambda$ ) of the measured CH<sub>3</sub>F absorption lines, with maximum error within the second decimal unit.

| $\nu'$ (cm <sup>-1</sup> ) | $\lambda$ (Å) | $\sigma_{\max}$ (10 <sup>-25</sup> cm <sup>2</sup> /molecule) | $\nu'$ (cm <sup>-1</sup> ) | $\lambda$ (Å) | $\sigma_{\max}$ (10 <sup>-25</sup> cm <sup>2</sup> /molecule) |
|----------------------------|---------------|---|----------------------------|---------------|---|
| 11 545.28                  | 8659.22       |   | 11 637.36                  | 8590.70       |   |
| 11 545.39                  | 8659.14       |   | 11 637.57                  | 8590.55       |   |
| 11 545.55                  | 8659.02       | 2.5 ± 0.5   | 11 637.66                  | 8590.48       | 0.8 ± 0.2   |
| 11 545.80                  | 8658.83       |   | 11 637.76                  | 8590.41       |   |
| 11 546.00                  | 8658.68       |   | 11 638.47                  | 8589.88       |   |
| 11 546.17                  | 8658.55       |   | 11 638.61                  | 8589.78       | 1.4 ± 0.3   |
| 11 546.37 <sup>a</sup>     | 8658.40       | 5.8 ± 0.2   | 11 646.32                  | 8584.09       | 0.4 ± 0.2   |
| 11 554.85                  | 8652.05       | 4.0 ± 0.2   | 11 647.37                  | 8583.32       | 1.2 ± 0.2   |
| 11 555.08                  | 8651.87       | 3.2 ± 0.2   | 11 652.94                  | 8579.22       |   |
| 11 564.73                  | 8644.66       | 2.6 ± 0.2   | 11 653.03                  | 8579.15       |   |
| 11 564.25                  | 8645.01       | 6.2 ± 0.4   | 11 653.15                  | 8579.06       |   |
| 11 571.88 <sup>b</sup>     | 8639.31       | 2.6 ± 0.2   | 11 653.28                  | 8578.97       |   |
| 11 581.24 <sup>b</sup>     | 8632.33       | 1.7 ± 0.3   | 11 653.39                  | 8578.89       |   |
| 11 583.56                  | 8630.60       | 3.2 ± 0.2   | 11 653.50                  | 8578.80       | 0.4 ± 0.1   |
| 11 583.81                  | 8630.42       | 1.7 ± 0.2   | 11 653.63                  | 8578.71       |   |
| 11 587.25                  | 8627.85       | 1.8 ± 0.2   | 11 653.68                  | 8578.67       |   |
| 11 587.38                  | 8627.76       | 1.2 ± 0.2   | 11 653.80                  | 8578.58       |   |
| 11 587.52                  | 8627.65       | 0.9 ± 0.2   | 11 653.88                  | 8578.52       |   |
| 11 587.63                  | 8627.57       | 2.5 ± 0.2   | 11 654.03                  | 8578.41       | 0.2 ± 0.1   |
| 11 588.27                  | 8627.09       |   | 11 654.54                  | 8578.04       |   |
| 11 588.34                  | 8627.04       | 0.3 ± 0.1   | 11 654.64                  | 8577.96       | 0.3 ± 0.1   |
| 11 558.45                  | 8626.96       |   | 11 655.02 <sup>a</sup>     | 8577.69       | 0.7 ± 0.2   |
| 11 588.93                  | 8626.60       | 2.7 ± 0.2   | 11 655.57                  | 8577.28       | 0.7 ± 0.1   |
| 11 597.28                  | 8620.39       |   | 11 663.71                  | 8571.29       | 0.5 ± 0.1   |
| 11 597.41                  | 8620.29       | 1.3 ± 0.2   | 11 664.42                  | 8570.77       | 0.8 ± 0.2   |
| 11 597.51                  | 8620.22       |   | 11 664.64                  | 8570.61       |   |
| 11 597.61                  | 8620.15       |   | 11 666.52                  | 8569.23       |   |
| 11 610.69                  | 8610.44       | 1.4 ± 0.2   | 11 666.58                  | 8569.12       | 0.6 ± 0.2   |
| 11 635.25                  | 8592.26       |   | 11 674.23 <sup>b</sup>     | 8563.57       | 1.2 ± 0.3   |
| 11 635.40                  | 8592.15       | 0.9 ± 0.2   | 11 677.00                  | 8561.54       | 4.9 ± 0.2   |
| 11 635.88                  | 8591.79       |   | 11 683.92                  | 8556.47       | 0.3 ± 0.1   |
| 11 636.00                  | 8591.71       |   | 11 692.81                  | 8549.96       | 0.3 ± 0.1   |
| 11 636.17                  | 8591.58       | 0.5 ± 0.2   | 11 694.26                  | 8548.90       |   |
| 11 636.30                  | 8591.49       |   | 11 694.34                  | 8548.84       |   |
| 11 636.56                  | 8591.29       |   | 11 694.60                  | 8548.65       | 0.6 ± 0.1   |
| 11 636.83                  | 8591.09       |   | 11 694.79                  | 8548.52       |   |
| 11 637.04                  | 8590.94       |   | 11 694.89                  | 8548.44       | 0.4 ± 0.1   |
| 11 637.16                  | 8590.85       | 0.3 ± 0.1   | 11 711.17                  | 8536.56       | 0.3 ± 0.1   |
| 11 637.26                  | 8590.78       |   | 11 711.82                  | 8536.09       |   |
| 11 713.09                  | 8535.16       |   | 11 762.58                  | 8499.25       |   |
| 11 713.22                  | 8535.07       |   | 11 767.83                  | 8495.46       | 0.2 ± 0.1   |
| 11 713.36                  | 8534.96       |   | 11 767.86                  | 8495.44       | 0.3 ± 0.1   |
| 11 713.74                  | 8534.69       |   | 11 768.92                  | 8494.67       |   |
| 11 713.98                  | 8534.51       |   | 11 769.02                  | 8494.60       |   |
| 11 714.82                  | 8533.90       | 0.5 ± 0.1   | 11 769.16                  | 8494.50       |   |
| 11 714.93                  | 8533.82       |   | 11 769.28                  | 8494.41       |   |
| 11 722.03                  | 8528.65       |   | 11 769.38                  | 8494.34       |   |
| 11 722.19                  | 8528.53       |   | 11 769.52                  | 8494.24       | 0.2 ± 0.2   |
| 11 722.31                  | 8528.45       | 0.7 ± 0.1   | 11 770.07                  | 8493.84       | 0.6 ± 0.1   |
| 11 722.41                  | 8528.37       |   | 11 770.26                  | 8493.70       |   |
| 11 731.56                  | 8521.72       | 0.6 ± 0.2   | 11 770.46                  | 8493.56       | 0.5 ± 0.2   |
| 11 732.96                  | 8520.71       | 0.3 ± 0.1   | 11 770.69                  | 8493.39       |   |
| 11 733.07                  | 8520.63       |   | 11 770.82                  | 8493.30       |   |
| 11 733.20                  | 8520.53       |   | 11 770.91                  | 8493.23       |   |
| 11 740.72                  | 8515.07       |   | 11 771.10                  | 8493.10       |   |
| 11 740.86                  | 8514.97       | 1.5 ± 0.2   | 11 771.59                  | 8492.74       | 0.6 ± 0.2   |
| 11 741.07                  | 8514.82       |   | 11 772.05                  | 8492.41       |   |
| 11 741.33                  | 8514.63       |   | 11 772.15                  | 8492.34       |   |
| 11 741.49                  | 8514.52       | 0.3 ± 0.1   | 11 772.27                  | 8492.25       | 0.4 ± 0.2   |
| 11 748.30                  | 8509.58       | 0.8 ± 0.2   | 11 772.58                  | 8492.03       | 0.8 ± 0.2   |
| 11 748.93                  | 8509.12       | 0.5 ± 0.2   | 11 773.10                  | 8491.65       |   |
| 11 749.04                  | 8509.04       |   | 11 773.22                  | 8491.57       |   |
| 11 749.24                  | 8508.90       |   | 11 773.54                  | 8491.34       |   |
| 11 749.37                  | 8508.80       |   | 11 773.76                  | 8491.18       | 0.5 ± 0.2   |
| 11 749.65                  | 8508.60       | 0.4 ± 0.1   | 11 777.84                  | 8488.24       |   |
| 11 758.32                  | 8502.33       | 0.5 ± 0.1   | 11 777.92                  | 8488.18       | 0.2 ± 0.1   |
| 11 759.64                  | 8501.37       | 0.2 ± 0.1   | 11 778.01                  | 8488.12       |   |
| 11 759.73                  | 8501.31       |   | 11 779.89                  | 8486.76       | 1.5 ± 0.2   |
| 11 759.82                  | 8501.24       |   | 11 795.51 <sup>b</sup>     | 8475.52       |   |

**Table 1** (continued)

| $\nu'$ (cm <sup>-1</sup> ) | $\lambda$ (Å) | $\sigma_{\max}$ (10 <sup>-25</sup> cm <sup>2</sup> /molecule) | $\nu'$ (cm <sup>-1</sup> ) | $\lambda$ (Å) | $\sigma_{\max}$ (10 <sup>-25</sup> cm <sup>2</sup> /molecule) |
|----------------------------|---------------|---|----------------------------|---------------|---|
| 11 759.89                  | 8501.19       |   | 11 797.29 <sup>b</sup>     | 8474.24       |   |
| 11 761.36                  | 8500.13       |   | 11 800.37 <sup>b</sup>     | 8472.03       | 1.0 ± 0.1   |
| 11 761.47                  | 8500.05       |   | 11 806.33                  | 8467.75       | 1.7 ± 0.5   |
| 11 761.56                  | 8499.99       |   | 11 829.55                  | 8451.13       | 1.6 ± 0.5   |
| 11 761.76                  | 8499.84       | 0.7 ± 0.1   | 11 830.19                  | 8450.67       | 0.1 ± 0.1   |
| 11 762.12                  | 8499.58       | 0.2 ± 0.1   | 11 834.78                  | 8447.40       | 0.1 ± 0.1   |
| 11 762.24                  | 8499.49       |   | 11 834.85                  | 8447.35       |   |
| 11 762.34                  | 8499.42       |   | 11 835.92                  | 8446.58       |   |
| 11 762.47                  | 8499.33       |   | 11 836.30                  | 8446.31       | 0.4 ± 0.1   |

<sup>a</sup> The wavenumbers marked are probably related to double lines.

<sup>b</sup> The wavenumbers marked are measured with respect to iodine.

**Table 2**  
Methyl fluoride absorption line strengths.

| $\nu'$ (cm <sup>-1</sup> ) | $S$ (10 <sup>-26</sup> cm/molecule) |
|----------------------------|-------------------------------------|
| 11 554.85                  | 2.4 ± 0.2                           |
| 11 564.25                  | 2.9 ± 0.2                           |
| 11 583.56                  | 1.3 ± 0.1                           |
| 11 588.93                  | 1.0 ± 0.1                           |
| 11 677.00                  | 1.9 ± 0.1                           |
| 11 779.89                  | 0.7 ± 0.1                           |
| 11 800.37                  | 0.4 ± 0.1                           |

**Table 3**  
CH<sub>3</sub>F pressure FWHM broadening ( $\gamma$ ) and shift coefficients ( $\delta$ ).

| $\nu'$ (cm <sup>-1</sup> ) | $\gamma_{\text{self}}$ | $\gamma_{\text{air}}$ (MHz/Torr) | $\delta_{\text{self}}$ (MHz/Torr) | $\delta_{\text{air}}$ (MHz/Torr) |
|----------------------------|------------------------|----------------------------------|-----------------------------------|----------------------------------|
| 11 554.85                  | 34 ± 1                 |                                  |                                   |                                  |
| 11 564.25                  | 22.7 ± 0.5             | 12 ± 1                           | -1.3 ± 0.2                        | 1.0 ± 0.8                        |
| 11 583.56                  | 11 ± 2                 |                                  |                                   |                                  |
| 11 588.93                  | 18 ± 1                 |                                  |                                   |                                  |
| 11 677.00                  | 9 ± 1                  | 6 ± 1                            |                                   |                                  |
| 11 779.89                  | 18 ± 3                 |                                  |                                   |                                  |
| 11 800.37                  | 12.2 ± 0.1             |                                  |                                   |                                  |

originated by the reflections inside the multipass cell: the distance between the fringes is  $\Delta\nu \approx 0.175$  GHz, and the distance between confocal mirrors inside the multipass cell was  $l = 42.8$  cm [ $\Delta\nu = c/(4l)$ ]. The F.-P. interferometer transmission is also shown as frequency marker. The étalon effect could be reduced by improving the LD beam collimation with the utilization of specific aspheric lenses, which will be one of the future improvements of this spectroscopy.

### 3. Experimental results

In Table 1 the detected absorption lines are listed. The very congested band observed could suggest a  $\perp$  type band [16]. The maximum absorption cross section ( $\sigma_{\max}$ ) is reported only where it could be measured by the direct absorption (DA) technique, as the WMS with high modulation amplitude can bring to big systematic errors in the absolute value of the absorbance. These measurements were performed at room temperature, at a pressure around 30 Torr and 30 m pathlength. The wavelengths are calculated in air at  $T = 294$  K following the work of Edlén [17]. As previously said, owing to the mode hops suffered by the LDs, this list cannot pretend to be exhaustive; anyhow in our knowledge this is the first time these lines have been accurately measured.

By assuming a Voigt line shape, we could integrate the absorption coefficient in energy to obtain the line strength with an acceptable error for seven of the more intense observed lines. The results are shown in Table 2.

With the modulation amplitude kept low, we measured the self-broadening coefficients of the FWHM for the seven lines at room temperature, and for two of them

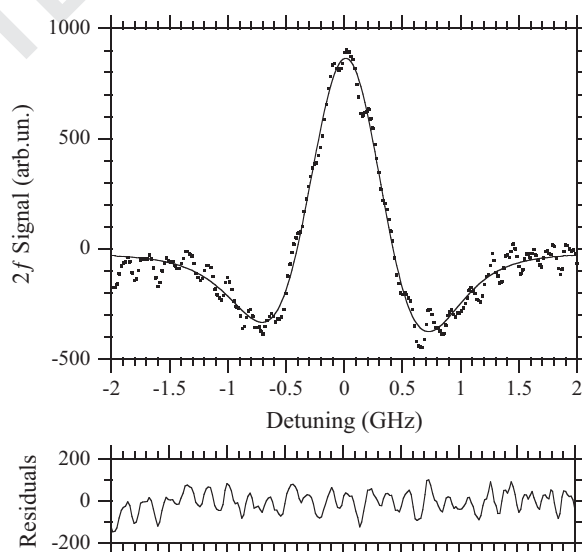


**Fig. 4.** Second derivative signal of the methyl fluoride absorption line at 11 564.25 cm<sup>-1</sup> along with its best fit and related residuals.

also the air-broadening ones. In this case the CH<sub>3</sub>F partial pressure was 20 Torr. Finally for the most intense line at 11 564.25 cm<sup>-1</sup> the shift coefficients could be obtained too. The results are reported in Table 3.

During the least square fitting procedure the Doppler component of the Voigt function was a constant parameter kept to the value calculated at the measurement conditions.



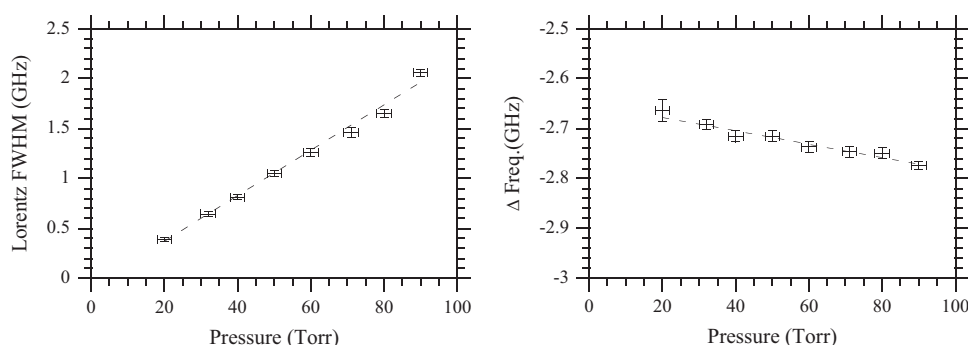


**Fig. 5.** Self-broadening (left) and self-shift (right) measurements for the 11 564.25  $\text{cm}^{-1}$  methyl fluoride absorption line as a function of its pressure at room temperature.

In Fig. 4 there is an example of the  $2f$  measurement of the 11 564.25  $\text{cm}^{-1}$  line at  $p_{\text{CH}_3\text{F}} = 32$  Torr,  $T = 294$  K, and 10 Hz band width, with low modulation amplitude. The fit function is the 2nd derivative of the Voigt function. The étalon effect is observable in the residuals.

A graphical example of one of the collisional broadening and shift measurements is shown in Fig. 5. On the left the Lorentz FWHM component of the 11 564.25  $\text{cm}^{-1}$  line shape is plotted as a function of the  $\text{CH}_3\text{F}$  pressure, while on the right the frequency difference ( $\Delta$  Freq.) between the  $\text{CH}_3\text{F}$  line and a reference line at a fixed known position is shown as a function of the methyl fluoride pressure. All the measurements were performed at room temperature. It is remarkable that, even if the shift effect was an order of magnitude lower than the broadening, it was still observable with acceptable errors. In particular, all the errors are always the maximum errors ( $3\sigma$ ), and for the pressure they were all within 1 Torr, while for the Lorentzian FWHM they came for the fit procedure and were principally affected by the above mentioned étalon effect.

In our knowledge no other pressure broadening and shift measurements can be found in the literature at these wavenumbers, therefore only a comparison with what obtained in different spectral regions can be done. As explained previously, this experimental work did not provide the quantum number classification of the single line, therefore here only an average comparison with what published by others can be tried.

Since the first self-broadening measurements performed in 1949 [18], results have been obtained in the microwave and in the infrared regions, ranging roughly between 10 and 40 MHz/Torr.

In the infrared region, self-broadening coefficients in the fundamental vibronic quantum  $\nu_6$  band have been measured by Leperè et al. [19] at 8.5  $\mu\text{m}$ , on average their values result higher than ours; in particular they used a different fit function, the Rautian profile, that takes into account the velocity-changing collision effects. In their case the line shifting was negligible.

This happens also when we compare our self-broadening results with the ones reported in the work of Lerota et al. [20] on the  $\nu_2$  and  $\nu_5$  bands between 6.5 and 7  $\mu\text{m}$  at room temperature.

A comparison can also be done with the results of the work on the fundamental  $\nu_2$  at 6.8  $\mu\text{m}$  [21] and two of our measurements, at 11 554.85 and 11 564.25  $\text{cm}^{-1}$ , are consistent with these results.

Still the self-broadening coefficient measured at 3.5  $\mu\text{m}$  by using a difference-frequency laser by the  $\text{LiNbO}_3$  nonlinear crystal and the Stark modulation technique [22] is similar to our result at 11 583.56  $\text{cm}^{-1}$ .

On the  $\nu_4$  band at 3.3  $\mu\text{m}$  also the self-broadening data of Cartledge and Butcher [23], obtained by a tunable laser source consisting of two parametric mixed lasers through a lithium niobate crystal, are aligned to our values.

Ikram et al. [24] by a  $\text{CO}_2$  Stark-tunable laser on the  $\nu_3 : ^0\text{Q}(1,1)$  transition at 9.5  $\mu\text{m}$  obtained  $\gamma_{\text{self}}^{\text{HWHM}} = (18.7 \pm 1.1)$  MHz/Torr, which is comparable to our result at 11 554.85  $\text{cm}^{-1}$ .

The self-broadening coefficients, and the self-shift in its absolute value, are also similar to the ones of Rohart et al. [25] in the millimeter wave range.

Finally, for what the air-broadening concerns, our results are aligned to what Guerin et al. [26] got in the  $\nu_2$  and  $\nu_5$  bands around 6.8  $\mu\text{m}$ .

#### 4. Conclusion

By using a tunable diode laser spectrometer 156 methyl fluoride overtone absorption lines have been detected by the aid of the wavelength modulation and the 2nd harmonic detection techniques. The line-shape parameters were obtained by fitting the observed signals with the standard Voigt profile through a **non-linear** least squares fitting program. For the more intense of them the absorption cross sections have been measured giving line strengths of the order of  $10^{-26}$ – $10^{-27}$   $\text{cm}^2/\text{molecule}$ . These absorption bands can only be detected by high sensitive techniques and very long path-lengths, in fact their extinction coefficients correspond to some tens of kilometers. For some of these lines the pressure broadening coefficients have been measured and for the most intense, pressure shift coefficients have been obtained too. Some comparisons with previous works, even if at different wavelengths, are consistent with our results.

## Acknowledgments

The authors wish to thank Mr. A. Barbini for the electronic advising and Mr. M. Tagliaferri for the technical assistance. We are indebted with Dr. S. Marchetti for his precious suggestions and for supplying the CH<sub>3</sub>F pure gas.

## References

- [1] Lucchesini A, Gozzini S. Collisional broadening and shifting of ammonia absorption lines at 790 nm. *Eur Phys J D* 2003;22:209–15.
- [2] Lucchesini A, Gozzini S. Diode laser spectroscopy of ammonia at 760 nm. *Opt Commun* 2009;282:3493–8.
- [3] Freund SM, Duxbury G, Römheld M, Tiedje JT, Oka T. Laser Stark spectroscopy in the 10  $\mu$ m region: the  $\nu_3$  bands of CH<sub>3</sub>F. *J Mol Spectrosc* 1974;52:38–57.
- [4] Sattler JP, Simonis GJ. Tunable diode laser spectroscopy of methyl fluoride. *IEEE J Quantum Electron* 1977;13:461–5.
- [5] Thompson HW. Vibration-rotation bands of some polyatomic molecules in the photographic infra-red. *J Chem Phys* 1939;7:441–7.
- [6] Wong JS, Moore CB. Inequivalent C–H oscillators of gaseous alkanes and alkenes in laser photoacoustic overtone spectroscopy. *J Chem Phys* 1982;77:603–15.
- [7] Law MM. Joint local- and normal-mode studies of the overtone spectra of the methyl halides: CH<sub>3</sub>F, CH<sub>3</sub>Cl, CH<sub>3</sub>Br, CD<sub>3</sub>Br, and CH<sub>3</sub>I. *J Chem Phys* 1999;111:10021–33.
- [8] Duncan JL, Law MM. A study of vibrational anharmonicity, Fermi resonance interactions, and local mode behavior in CH<sub>3</sub>Cl. *J Mol Spectrosc* 1990;140:13–30.
- [9] Champion JP, Robiette AG, Mills IM, Graner G. Simultaneous analysis of the  $\nu_1$ ,  $\nu_4$ ,  $2\nu_2$ ,  $\nu_2 + \nu_5$ , and  $2\nu_5$  infrared bands of <sup>12</sup>CH<sub>3</sub>F. *J Mol Spectrosc* 1982;96:422–41.
- [10] Lucchesini A, Gozzini S. Methane diode laser overtone spectroscopy at 840 nm. *J Quant Spectrosc Radiat Transfer* 2007;103:209–16.
- [11] (<http://www.scintec.it>).
- [12] Rothman LS, Gordon IE, Barbe A, Benner DC, Bernath PF, Birk M, et al. The HITRAN 2008 molecular spectroscopic database. *J Quant Spectrosc Radiat Transfer* 2009;110:533–72.
- [13] Gerstenkorn S, Verges S, Chevillard J. Atlas du spectre d'absorption de la molécule d'iode. Lab Aimé Cotton, Orsay, France: Edition du CNRS; 1982.
- [14] Dicke RH. The effect of collisions upon the Doppler width of spectral lines. *Phys Rev* 1953;89:472–3.
- [15] De Rosa M, Ciucci A, Pelliccia D, Gabbanini C, Gozzini S, Lucchesini A. On the measurement of pressure induced shift by diode lasers and harmonic detection. *Opt Commun* 1998;147:55–60.
- [16] Bennett WH, Meyer CF. The infra-red absorption spectra of the methyl halides. *Phys Rev* 1928;32:888–905.
- [17] Edlén B. The refractive index of air. *Metrologia* 1966;2:71–80.
- [18] Gilliam OR, Edwards HD, Gordy W. Microwave investigations of methyl fluoride, fluorocform, and phosphorus trifluoride. *Phys Rev* 1949;75:1014–6.
- [19] Lepère M, Blanquet G, Walrand J, Bouanich J-P. Line intensities in the  $\nu_6$  band of CH<sub>3</sub>F at 8.5  $\mu$ m. *J Mol Spectrosc* 1996;180:218–26.
- [20] Lerot C, Blanquet G, Bouanich J-P, Walrand J, Lepère M. Self-broadening coefficients in the  $\nu_2$  and  $\nu_5$  bands of <sup>12</sup>CH<sub>3</sub>F at 183 and 298 K. *J Mol Spectrosc* 2005;230:153–60.
- [21] Wilkinson KA, Aoaeh BL, Bhattarai S, Khan RA, Mantz AW. Self broadening and linestrength determinations in the  $\nu_2$  and  $\nu_5$  bands of CH<sub>3</sub>F. *Spectrochim Acta A: Mol Biomol Spectrosc* 1999;55:2039–48.
- [22] Brechignac Ph. Reorientation and pressure broadening of IR or MW lines: new results in CH<sub>3</sub>F. *J Chem Phys* 1982;76:3389–95.
- [23] Cartlidge AG, Butcher RJ. Self-broadening of transitions in the  $\nu_4$  3  $\mu$ m band of CH<sub>3</sub>F using a difference frequency laser. *J Phys B: At Mol Opt Phys* 1990;23:2083–90.
- [24] Ikram M, Butcher RJ. Saturation dip measurements of pressure broadening in CH<sub>3</sub>F. *J Phys B: At Mol Opt Phys* 1991;24:943–9.
- [25] Rohart F, Ellenendt A, Kaghat F, Mäder H. Self and polar foreign gas line broadening and frequency shifting of CH<sub>3</sub>F: effect of the speed dependence observed by millimeter-wave coherent transients. *J Mol Spectrosc* 1997;185:222–33.
- [26] Guerin D, Nischan M, Clark D, Dunjko V, Mantz AW. Low-pressure measurements of self and air broadening coefficients in the  $\nu_2$  and  $\nu_5$  bands of <sup>12</sup>CH<sub>3</sub>F. *J Mol Spectrosc* 1994;166:130–6.